*Key Engineering Materials*
*ISSN: 1662-9795, Vol. 1050, pp 145-155*
*doi:10.4028/p-M2Pzus*

*Submitted: 2026-01-19*
*Revised: 2026-02-16*
*Accepted: 2026-02-26*
*Online: 2026-04-16*

# A Bayesian Data Assimilation Framework for Characterizing Recrystallization in Steels

Bentolhoda Jamshidi[1,a*], Jos Havinga[1,b], and Ton van den Boogaard[1,c]

[1] Faculty of Engineering Technology, University of Twente, The Netherlands

[a]b.jamshidi@utwente.nl, [b]jos.havinga@utwente.nl, [c]a.h.vandenboogaard@utwente.nl

**Keywords:** Recrystallization, Bayesian Data Assimilation, Particle Filter, Sequential Monte Carlo, Steels

**Abstract.** In this study, we develop a Bayesian data assimilation framework that combines a mean-field model of static recrystallization (MiReX) with a Sequential Importance Resampling (SIR) particle filter to estimate key material parameters from controlled synthetic experiments. MiReX, originally developed as a microstructurally based extension of Johnson–Mehl–Avrami–Kolmogorov kinetics, is used as a forward model in which the uncertain quantities include the grain-boundary mobility parameters (prefactor and activation energy), a stored-energy coefficient, an Avrami-type exponent, and an interface length scale. Synthetic recrystallized-fraction measurements are generated at two isothermal holding temperatures using a reference parameter set and are perturbed with Gaussian noise to mimic experimental uncertainty. Starting from broad uniform prior ranges, the particle filter propagates an ensemble of MiReX trajectories in time, updates particle weights using a Gaussian likelihood, and applies systematic resampling combined with Liu–West kernel regularization to reduce particle degeneracy while preserving posterior variance. The posterior obtained after assimilating the first temperature dataset is used as the prior for the second dataset, enabling sequential multi-temperature calibration. The synthetic experiments show that the framework recovers the reference parameters within credible intervals and provides tight uncertainty bounds on the predicted recrystallization kinetics. These results demonstrate that combining a physically based mean-field recrystallization model with sequential Monte Carlo methods provides a robust route for probabilistic parameter estimation and uncertainty quantification in microstructure evolution models.

## Introduction

Static recrystallization plays a central role in controlling grain structure and mechanical properties of metals during thermo-mechanical processing. Reliable prediction of recrystallization kinetics and microstructural evolution is therefore crucial for optimizing industrial operations such as rolling, forging, and annealing. To this end, a wide range of models has been proposed, ranging from phenomenological mean-field approaches to spatially resolved phase-field simulations. The capability of these models to capture actual recrystallization kinetics depends on the modeling assumptions (e.g. averaging in mean-field approaches versus full field predictions in phase-field simulations) and on the accuracy of the internal physical model parameters. Although these models are commonly used in a deterministic setting, the uncertainty in the predictions may be significant due to the assumptions and uncertain model parameters. In this work, a mean-field recrystallization model is therefore used in a stochastic (i.e. Bayesian) framework, in which uncertain model parameters are estimated in probabilistic terms using experimental measurements. The rationale of the approach is that measurable quantities that are affected by model parameters can be used to reduce model parameter uncertainty and improve model predictions, even if no unique solution to the inverse parameter problem exists.

The multi-phase-field (MPF) method is a powerful tool for modeling recrystallization because it explicitly resolves grain-boundary migration and complex microstructural morphologies. However, its predictive capability is often limited by uncertainties in key parameters such as grain-boundary mobility, grain-boundary energy, and stored-energy distributions, which are difficult to measure experimentally and may vary spatially. In addition, MPF simulations are computationally expensive,

particularly when combined with uncertainty quantification or data-assimilation techniques. Bayesian approaches have recently been introduced to improve MPF-based modeling. Seguchi et al. employed an ensemble Kalman filter (EnKF) to estimate phase-field simulation parameters, including interface mobility and gradient energy coefficients, during eutectic alloy solidification [1], while Yamanaka et al. extended this framework to three-dimensional MPF simulations to identify anisotropic grain-boundary energy and mobility functions using EnKF-based data assimilation [2]. Further developments include Bayesian estimation of anisotropic grain-boundary energies and mobilities for multiple boundary types by Miyoshi et al. [3], and molecular-dynamics-informed phase-field modeling to extract inclination-dependent grain-boundary energies by Fujiwara et al. [4].

Bayesian data assimilation has also been successfully applied to other microstructure evolution processes. Ishii et al. combined in situ electron tomography with Bayesian assimilation to identify temperature-dependent diffusion coefficients in phase-field sintering simulations [5]. In solidification studies, Ohno et al. used Bayesian inference and EnKF-based methods to estimate solid–liquid interfacial properties from atomistic and phase-field simulations [6]. Beyond phase-field models, Bayesian frameworks have been applied to calibrate constitutive and mechanistic models. Honarmandi and Arroyave used Markov chain Monte Carlo methods to calibrate strain–stress models for TRIP steels, demonstrating Bayesian inference's ability to quantify uncertainty and reveal parameter correlations [7]. These studies contribute to the increasing use of Bayesian uncertainty quantification and data assimilation in nonlinear dynamical systems. Works by van Leeuwen [8], Fearnhead and Künsch [9] , and the monograph by Grudzien and Bocquet [10] provide the theoretical basis for particle filters, ensemble Kalman methods, and generative-model-based inference. Applications continue to expand, including Bayesian estimation for recovery of elasto-plastic constitutive parameters using particle filters [11] and online Bayesian monitoring of thin-film growth during pulsed-laser deposition [12].

Alongside these developments, mean-field recrystallization models such as MiReX offer a computationally efficient alternative to MPF simulations. Based on extended Johnson–Mehl–Avrami–Kolmogorov kinetics, MiReX describes the temporal evolution of recrystallized volume fraction using physically meaningful parameters such as stored energy, grain-boundary mobility, temperature, and composition [13]. Although it does not explicitly resolve microstructure, its efficiency and interpretability make it well suited for parameter estimation and Bayesian data assimilation.

Bayesian inference provides a natural framework for parameter identification within MiReX by yielding full posterior distributions rather than single-point estimates. Sequential Monte Carlo methods, and in particular the Sequential Importance Resampling (SIR) particle filter, are well suited for the nonlinear and non-Gaussian nature of recrystallization kinetics. Particle filters can be used to evolve ensembles of states and parameters in time, assimilating recrystallization observations in a manner analogous to successful Bayesian estimation in phase-field models [1–6].

In this work, we present a Bayesian data-assimilation framework that couples the MiReX mean-field model with an SIR particle filter for parameter estimation in static recrystallization. A synthetic-experiment approach is adopted to assess the performance of the inversion method: synthetic recrystallized fraction data F(t) are generated using known model parameters and perturbed with Gaussian noise to mimic experimental uncertainty. The particle filter estimates key parameters governing recrystallization, including the mobility prefactor, grain-boundary activation energy, stored energy, Avrami exponent, and interface radius. Synthetic experiment data is generated at two isothermal temperatures, with posterior distributions propagated across temperatures to assess parameter consistency. A Liu–West shrinkage kernel is employed to reduce particle degeneracy. The paper is organized as follows. Section MiReX-based forward model and synthetic-experiment design describes the MiReX model and the synthetic-experiment design. Section Bayesian data assimilation with Sequential Importance Resampling presents the Bayesian data-assimilation methodology. Section Results presents the numerical results. Section Discussion and Conclusion discusses the implications and limitations of the study.

### MiReX-Based Forward Model and Synthetic-Experiment Design

We adopt a MiReX-inspired mean-field model as proposed by Mathevon et al. [13], that describes the time evolution of the recrystallized volume fraction $F(t)$ under a varying temperature profile. In the original MiReX formulation, the recrystallized fraction is expressed as

$$F_{\text{Rex}}(t) = 1 - \exp\left(-F_{\text{Ext}}(t)\right), \tag{1}$$

where $F_{\text{Ext}}(t)$ is the extended fraction that accounts for nucleation and growth events and is typically written as

$$F_{\text{Ext}}(t) = N_{\text{Rex}} \left( \int_0^t M(T(\tau), X) G_{\text{Rex}}(\tau) d\tau \right)^{n_A}, \tag{2}$$

with $N_{\text{Rex}}$ being the effective nucleation-site density, $M(T, X)$ the effective grain-boundary mobility (function of temperature $T$ and composition $X$), $G_{\text{Rex}}$ the driving pressure for recrystallization (i.e. the internal strain energy), and $n_A$ the Avrami exponent describing growth geometry. $N_{\text{Rex}}$ is related to an interaction length scale $R_{\text{int}}$ and the Avrami exponent $n_A$ as below:

$$N_{\text{Rex}} = \left( \frac{1}{R_{\text{int}}} \right)^{n_A}. \tag{3}$$

The effective mobility $M$ is modeled as a segregation-corrected mobility derived from a Cahn-type description of solute drag. The "pure" mobility $M_{\text{pure}}$ is defined as

$$M_{\text{pure}}(T) = \frac{C_M}{RT} \exp\left( -\frac{Q_{\text{gb}}}{RT} \right), \tag{4}$$

where $Q_{\text{gb}}$ is the grain-boundary activation energy, $R$ is the gas constant, and $C_M$ is a mobility prefactor. The constant $C_M$ is a composite mobility prefactor defined as

$$C_M = \beta \, \frac{V_m \, \delta}{b^2} \, D^0_{gb}, \tag{5}$$

grouping the grain-boundary diffusivity prefactor $D^0_{gb}$, grain-boundary thickness $\delta$, atomic spacing via the Burgers vector $b$, and the molar volume of ferrite $V_m$. Solute drag is incorporated through an effective segregation factor that accounts for the combined influence of alloying elements. Each coefficient $\alpha_i$ represents a solute-dependent mobility slowdown coefficient, computed from nominal segregation parameters and the temperature $T$. The effective grain-boundary mobility is therefore written as

$$M = \frac{M_{\text{pure}}}{1 + M_{\text{pure}} \sum_{i=1}^{n} \alpha_i X_i}. \tag{6}$$

In the present synthetic experiments, the nominal composition and solute-drag parameters are fixed, and uncertainty is concentrated in $C_M$ and $Q_{\text{gb}}$, which control the overall magnitude and temperature sensitivity of $M$.

To construct synthetic experiments, a reference parameter set is chosen:

$$\theta_{\text{true}} = (C_M^{\text{true}}, Q_{\text{gb}}^{\text{true}}, G^{\text{true}}, n_A^{\text{true}}, R_{\text{int}}^{\text{true}}), \tag{7}$$

informed by previous MiReX calibrations for high-strength steels. In the simulations presented here, the true values are [13]

$$\begin{aligned} &C_M^{\text{true}} = 12.1, && G^{\text{true}} = 6.98 \times 10^5 \text{J/m}^3, && n_A^{\text{true}} = 1.3, \\ &R_{\text{int}}^{\text{true}} = 8.0 \times 10^{-6} \text{m}, && Q_{\text{gb}}^{\text{true}} = 148 \text{kJ/mol}. \end{aligned} \tag{8}$$

Synthetic data is generated in this study, corresponding to two distinct isothermal annealing experiments, with synthetic measurements taken at the following observation times:

$$\begin{aligned} t_1^1 &= 200\text{ s}, \quad t_2^1 = \ 500\text{ s}, \quad t_3^1 = 1000\text{ s} \quad \text{for} \quad T_1 = 923\text{ K} \\ t_1^2 &= 500\text{ s}, \quad t_2^2 = 1000\text{ s}, \quad t_3^2 = 2000\text{ s} \quad \text{for} \quad T_2 = 873\text{ K} \end{aligned} \tag{9}$$

For each temperature, the nominal segregation parameters and diffusion coefficients are adjusted, leading to different effective mobilities.

At each temperature, the forward model is integrated from $t = 0$ with the true parameters $\theta_{\text{true}}$ to obtain the noiseless recrystallized fraction $F_{\text{true}}(t_k, T)$. Synthetic observations are then generated as

$$y_k = F_{\text{true}}(t_k, T) + \varepsilon_k, \tag{10}$$

where $\varepsilon_k$ is Gaussian noise with zero mean and standard deviation $\sigma_{\text{meas}}$. These synthetic datasets form the basis of the synthetic experiments used to evaluate the particle-filter-based parameter estimation framework.

**Bayesian Data Assimilation with Sequential Importance Resampling**

We formulate the MiReX model into a state-space form suitable for particle filtering. The state vector at time $t_k$ is

$$\mathbf{x}_k = \left[F_{rex}(t_k),\ C_M,\ Q_{\text{gb}},\ G,\ n_A,\ R_{\text{int}}\right], \tag{11}$$

where $F_{rex}(t_k)$ is the time-evolving recrystallized fraction and the remaining entries are constant model parameters that are treated as time-invariant random variables. The system dynamics can be written as

$$x_k = f(x_{k-1}, \Delta t_k) + v_k, \tag{12}$$

where $f$ represents one MiReX time increment as defined by Eqs. (1) and (2), with time increments $\Delta t_k = t_k - t_{k-1}$ defined by the observations times given in Eq. (9). In the synthetic experiments, process noise is neglected ($v_k = 0$), so uncertainty arises only from the prior and measurement noise. Observations are perturbed by Gaussian noise $\varepsilon_k \sim \mathcal{N}(0, \sigma^2_{\text{meas}})$, yielding the measurement likelihood

$$p\left(y_k \mid x_k\right) = \frac{1}{\sqrt{2\pi}\,\sigma_{\text{meas}}} \exp\left[-\frac{\left(y_k - F_{rex}(t_k)\right)^2}{2\,\sigma^2_{\text{meas}}}\right], \tag{13}$$

where $y_k$ is the measured recrystallized at time $t_k$ fraction and $F_{rex}(t_k)$ is the estimated recrystallized fraction. The posterior distribution $p\left(x_k \mid y_{1:k}\right)$ is approximated using an ensemble of $N_s$ particles $\left\{x_k^{(i)},\ w_k^{(i)}\right\}_{i=1}^{N_s}$, such that

$$p\left(x_k \mid y_{1:k}\right) \approx \sum_{i=1}^{N_s} w_k^{(i)}\,\delta\left(x_k - x_k^{(i)}\right), \tag{14}$$

where $\delta(\cdot)$ is the Dirac delta distribution. In the prediction step, each particle is propagated deterministically:

$$x_k^{(i)} = f(x_{k-1}^{(i)}, t_k). \tag{15}$$

Upon receiving observation $y_k$, particle weights are updated using the measurement likelihood:

$$\tilde{w}_k^{(i)} = w_{k-1}^{(i)}\,p\left(y_k \mid x_k^{(i)}\right), \tag{16}$$

and then normalized,

$$w_k^{(i)} = \frac{\tilde{w}_k^{(i)}}{\sum_{j=1}^{N_s} \tilde{w}_k^{(j)}}. \tag{17}$$

A point estimate of the state can be obtained after each observation as the weighted mean of the particle set:

$$\hat{x}_k = \sum_{i=1}^{N_s} w_k^{(i)}\, x_k^{(i)}. \tag{18}$$

After each measurement step, resampling of the particles is performed, generating a new set of particles with equal weights without changing the probability distribution of the state vector. To prevent particle impoverishment associated with static parameters, Liu–West regularization is employed. The parameter vector

$$\theta = (C_M,\ Q_{gb},\ G,\ n_A,\ R_{int})\,, \tag{19}$$

is shrunk towards the ensemble mean with added Gaussian perturbations to maintain ensemble spread:

$$\theta_{\text{new}}^{(i)} = a\,\theta^{(i)} + (1-a)\,\bar{\theta} + \sqrt{1-a^2}\,z^{(i)}, \tag{20}$$

where $z^{(i)} \sim \mathcal{N}(0, S)$ and $S$ denotes the sample covariance matrix of the parameter ensemble. In practice, $z^{(i)}$ is generated as $z^{(i)} = L_c \xi^{(i)}$, with $\xi^{(i)} \sim \mathcal{N}(0, I)$ and $L_c L_c^{\top} = S$. The coefficient $a$ determines the amount of Liu-West regularization, with values of $a \leq 1$, and $a = 1$ corresponding to no regularization. The coefficient $a$ is initialized at a value of $a_1 = 0.98$, and after each Liu-West update the coefficient is changed with $a_i = 1 - 0.8 \cdot (1 - a_{i-1})$, such that it converges towards $a = 1$, meaning that the amount of Liu-West regularization reduces over particle filter updates. After Liu-West perturbation, the parameters are constrained within prior bounds, preserving approximate first and second moments of the distribution. At the initial temperature (923 K), uniform priors are assigned:

$$\begin{aligned}
C_M &\sim U(2.42,\, 60.52),\\
Q_{\text{gb}} &\sim U(1.0\times10^{5},\, 2.5\times10^{5})\ \text{J/mol},\\
G &\sim U(1.0\times10^{5},\, 3.0\times10^{6})\ \text{J/m}^3,\\
n_A &\sim U(0.8,\, 2.2),\\
R_{\text{int}} &\sim U(4.0\times10^{-6},\, 1.2\times10^{-5})\ \text{m}.
\end{aligned} \tag{21}$$

The initial recrystallized fraction is set to $F_{\text{Rex}}(0) = 0$, and particles are initialized by independent sampling from the priors. After assimilation at one temperature, the final posterior ensemble is used as an empirical prior for the next temperature, with $F_{\text{Rex}}$ set to zero. This strategy treats each temperature as a separate experiment sharing the same underlying parameters but different thermodynamic conditions.

## Results

To assess the proposed Bayesian particle-filtering framework, synthetic experiments were conducted using the MiReX model of static recrystallization. Synthetic recrystallization curves were generated at two annealing temperatures, $T_1$=923K, $T_2$=873K, using the reference MiReX parameter set and alloy composition for dual-phase steel ($X_{\text{Mn}}$=0.015, $X_{\text{Cr}}$=0.005, $X_{\text{Si}}$=0.003). This ensures that the true parameters are physically consistent with a realistic material system.

At each temperature, the reference parameters $\{C_M,\, Q_{\text{gb}},\, G,\, n_A,\, R_{\text{int}}\}$ were used to generate recrystallized fraction curves $F_{\text{Rex}}(t)$. Synthetic observations were obtained by sampling these curves

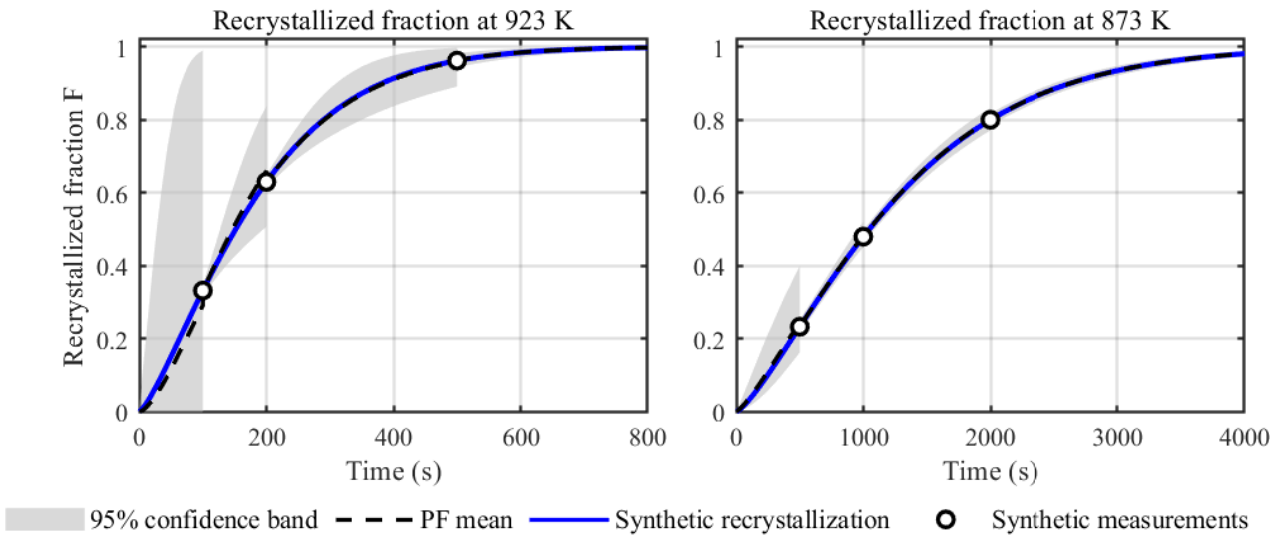


Fig. 1: Reconstructed recrystallized fraction $F_{\mathrm{Rex}}(t)$.

at realistic time points and adding Gaussian measurement noise with standard deviation $\sigma_{\mathrm{meas}}$=0.01. Since the true parameters are known, the resulting synthetic dataset provides a controlled benchmark for evaluating parameter identifiability, convergence, and multi-temperature consistency.

**Reconstruction of recrystallization kinetics and filter stability.** Figure 1 shows the reconstructed recrystallized fraction $F_{\mathrm{Rex}}(t)$ at the two temperatures. The particle ensemble accurately captures both the rapid increase of $F_{\mathrm{Rex}}(t)$ and its saturation towards $F_{\mathrm{Rex}} \approx 1$. After only a few observations, the 95% credible intervals become narrow, and the posterior mean and median closely match the noisy synthetic data, indicating rapid convergence of the particle filter despite broad initial parameter priors.

The filter is first applied at the higher temperature $T_1$, starting from wide and uninformative parameter ranges, which leads to a large uncertainty before the first measurements are available. After each measurement update, the particle ensemble correctly matches the observed recrystallized fraction. Between measurements, the prediction uncertainty increases again due to remaining uncertainty in the model parameters. The final estimate obtained at $T_1$ is then used as the initial condition for the analysis at the lower temperature $T_2$, rather than restarting the filter. At the beginning of $T_2$, the model response is still uncertain because the temperature has changed, but the filter quickly adjusts as new data are added. As more measurements are included, the uncertainty bands become narrower and the model prediction follows the synthetic reference curve more closely. This shows that using recrystallization data from multiple temperatures helps reduce parameter uncertainty and leads to more reliable predictions.

**Temperature-dependent evolution of parameter posteriors.** Figure 2 shows the evolution of posterior probability density functions (PDFs) for the five unknown MiReX parameters after ensemble update with the two temperatures, with vertical dashed lines indicating the reference values. As data from successive temperatures are assimilated in a sequential manner, the parameter estimates continue to narrow with added observations.

For the mobility prefactor $C_M$,the posterior initially spans nearly the full prior range at 923 K but narrows a bit as additional temperature data are included.

Single-temperature assimilation for the activation energy $Q_{\mathrm{gb}}$ leaves a broad posterior due to the well-known trade-off between prefactor and activation energy, but multi-temperature data sharply constrain $Q_{\mathrm{gb}}$. This reflects the fact that the Arrhenius mobility relation in Eq. (4) can be matched

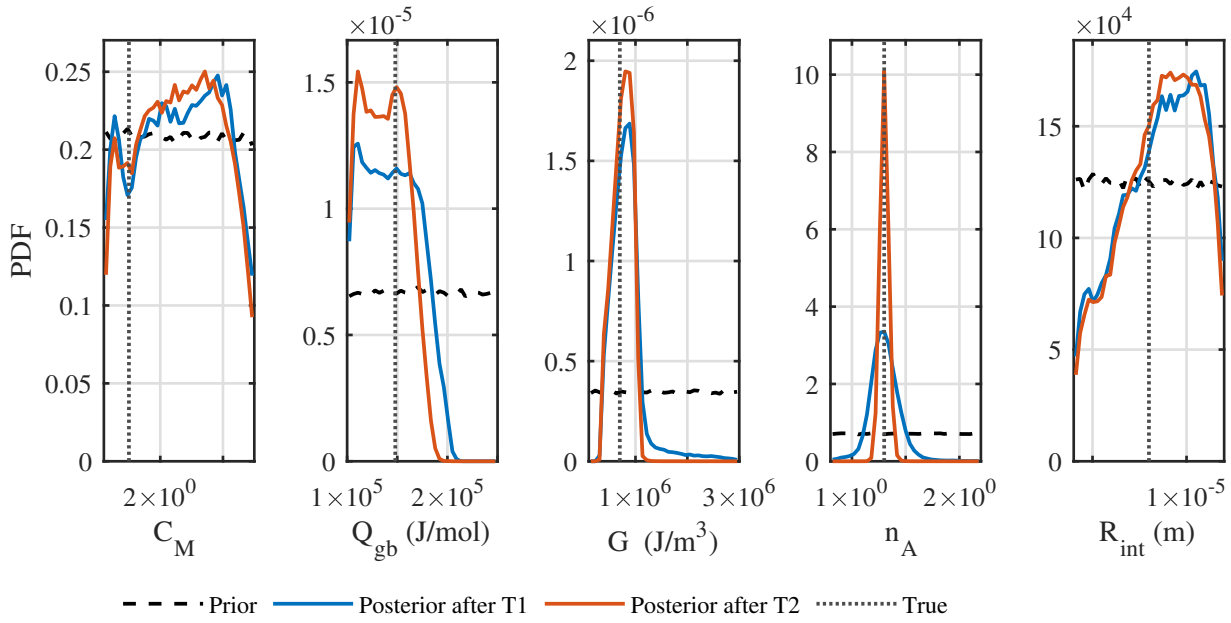


Fig. 2: Posterior probability density functions of MiReX parameters after sequential assimilation of multi-temperature measurements .

across multiple temperatures by a narrower set of ($C_M$,$Q_{\text{gb}}$) pairs, thereby breaking the degeneracy present in single-temperature fits.

The stored energy $G$ exhibits large reduction in uncertainty, with substantial narrowing of the distribution after the observations at $T_1$ are processed and additional narrowing after processing the observations at $T_2$. The Avrami exponent $n_A$ converges rapidly to a narrow interval around its reference value, indicating that the transformation-curve shape is strongly constrained by the data. In contrast, the interface length $R_{\text{int}}$ remains less well identified than most other parameters, retaining a broader credible interval due to its weaker influence on the observable kinetics.

Overall, the results demonstrate that multi-temperature assimilation yields robust parameter convergence, reduced uncertainty, and improved identifiability compared to single-temperature analysis.

**Joint parameter structure.** To analyze parameter relationships, the joint posterior distributions of parameter pairs were examined. Figure 3 shows pairwise posterior maps for the five MiReX parameters after assimilating data at $T_1$ and at $T_2$. The color intensity represents probability density, and the reference parameter set is marked by a cross. From $T_1$ to $T_2$, the posteriors generally tighten, showing improved parameter identification when the $T_2$ dataset is included. Notably, $Q_{\text{gb}}$ becomes strongly concentrated near its reference value, while $C_M$ remains relatively broad, indicating weaker identifiability of $C_M$. In contrast, the ($G$,$R_{\text{int}}$) plane exhibits a persistent positive correlation, which becomes very narrow at $T_2$, implying that these parameters remain strongly coupled and are not independently constrained. Overall, the $T_2$ assimilation yields tighter posteriors but also reveals remaining parameter couplings, especially involving $R_{\text{int}}$.

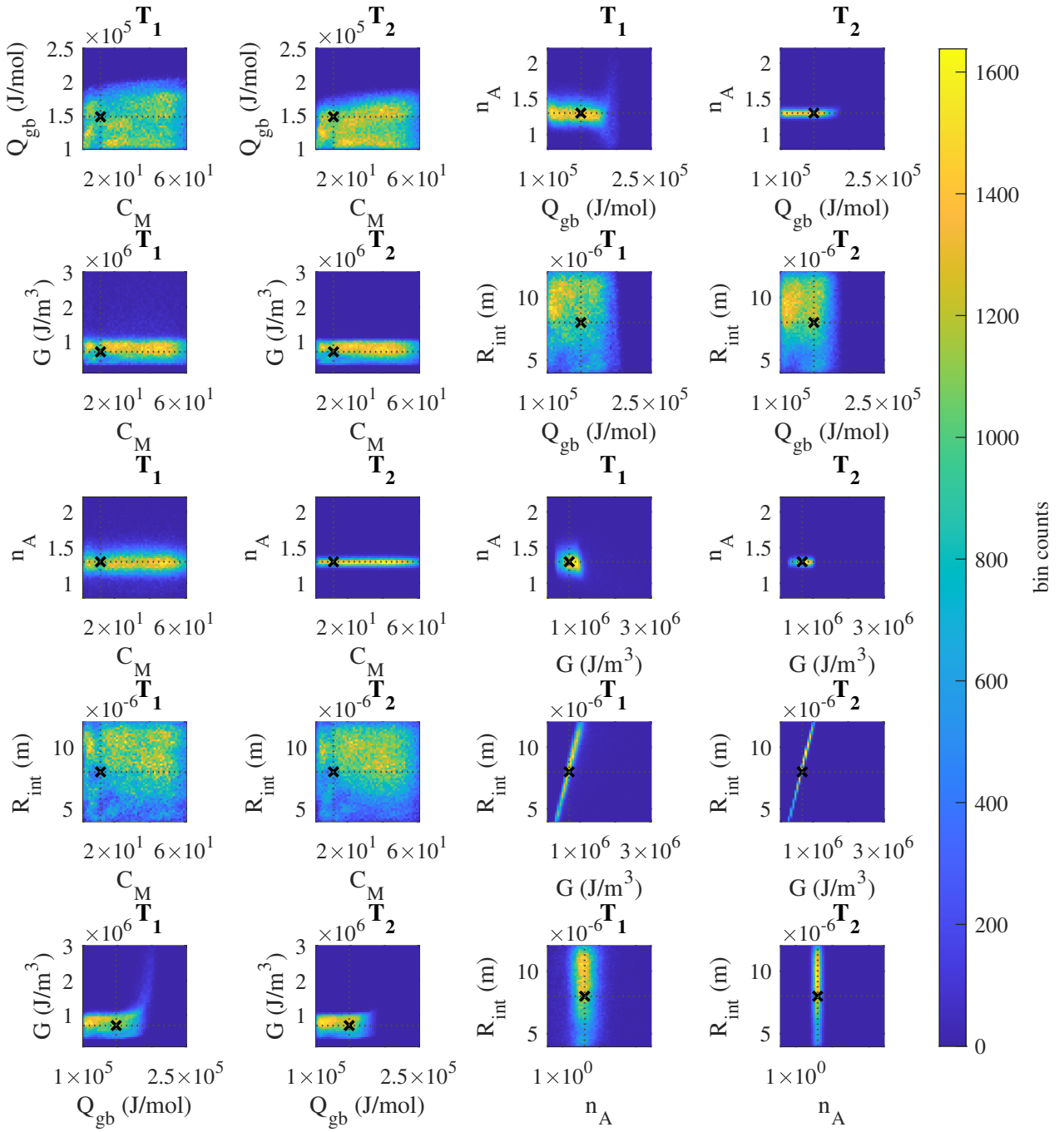


Fig. 3: Pairwise density plots of all parameter pairs ($C_M$, $Q_{\text{gb}}$, $G$, $n_A$, $R_{\text{int}}$) for the prior and posteriors after $T_1$ and $T_2$.

**Generalization of the particle filter to non-isothermal conditions.** So far, two constant temperatures, denoted as $T_1$ and $T_2$, were used to quantify uncertainty in the model parameters through sequential data assimilation. To test the generalization of the particle filter (PF) model beyond isothermal conditions, an arbitrary, non-constant temperature profile was considered. Figure 4(a) shows the applied temperature history, with dashed lines indicating $T_1$ and $T_2$. Figure 4(b) and Figure 4(c) show the predicted evolution of the recrystallized fraction after assimilation at $T_1$ and after sequential assimilation at both $T_1$ and $T_2$ , respectively. When only data from $T_1$ is used, the prediction shows larger uncertainty, while using data from both $T_1$ and $T_2$ reduces the uncertainty and improves the prediction.

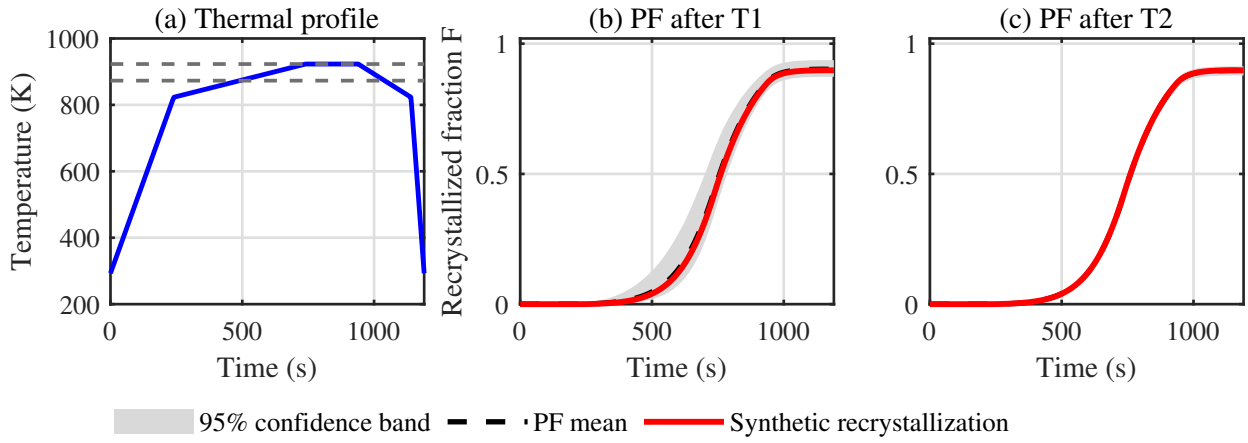


Fig. 4: An arbitrary thermal profile and the evolution of the recrystallized fraction estimated after sequential data assimilation steps .

## Discussion and Conclusion

This study presented a Bayesian data-assimilation framework that combines the MiReX mean-field model of static recrystallization with a Sequential Importance Resampling (SIR) particle filter using Liu–West regularization. The method was tested using synthetic data at multiple constant temperatures, with only a limited number of recrystallization measurements available at each temperature.

The results show that the framework can constrain the main MiReX parameters $C_M$, $Q_{\mathrm{gb}}$, $G$, $n_A$, and $R_{\mathrm{int}}$ starting from broad prior ranges. Instead of producing a single exact solution, the Bayesian approach provides parameter distributions that explicitly quantify the remaining uncertainty. The results indicate that different combinations of $C_M$, $Q_{\mathrm{gb}}$, $G$, $n_A$, and $R_{\mathrm{int}}$ can lead to very similar recrystallization curves for the available observations, confirming that the inverse identification problem is not unique.

**Scope, identifiability, and limitations of Bayesian parameter estimation.** The proposed framework performs Bayesian parameter estimation, meaning that the inferred parameter distributions are conditional on the assumed observation model, the measurement-noise model, and the MiReX mean-field formulation. As a consequence, parameter identifiability depends both on the experimental design and on the model structure.

A key result of this work is the benefit of using data from more than one temperature, especially when only a small number of measurements is available. Data from a single temperature mainly constrain the overall transformation speed but cannot clearly separate the effects of the mobility prefactor $C_M$ and the activation energy $Q_{\mathrm{gb}}$. By using data from $T = 923\,\mathrm{K}$ and $T = 873\,\mathrm{K}$ in sequence, the temperature dependence of the kinetics helps reduce uncertainty in both parameters. This shows that changing the temperature provides additional information, although some parameter coupling remains.

The analysis of parameter correlations gives further insight into which parameters can be identified. A strong correlation between $C_M$ and $Q_{\mathrm{gb}}$ reflects their combined role in the temperature-dependent mobility. Although using multiple temperatures improves the estimation of these parameters, a clear correlation remains between the driving force $G$ and the interface length $R_{\mathrm{int}}$. This indicates that these two parameters have similar effects on the recrystallization behavior and cannot be fully separated using only recrystallized-fraction data. Additional observables, such as recrystallized grain size, nucleus density, or texture measurements, would likely improve identifiability.

The reported credible intervals are conditional on the assumed measurement-noise model. Increasing measurement noise or reducing the number of observations would broaden the posterior distribu-

tions and reduce the ability to separate correlated parameters. For real experiments, the measurement uncertainty should therefore be estimated carefully, and the choice of likelihood model should reflect the characteristics of the experimental data.

Another important limitation is related to model representativity. The inferred parameters are conditional on the validity of the MiReX mean-field formulation. If the real material behavior includes effects that are not represented in the model, such as spatial heterogeneity in stored energy, variations in nucleation behavior, or grain-boundary character effects, Bayesian calibration may compensate for model mismatch by shifting parameters away from their true physical values. In practical applications, this issue can be addressed by comparing posterior predictions with independent measurements and by explicitly evaluating model discrepancies.

Several safeguards were used in the present work to reduce the risk of misleading parameter identification. First, multi-temperature assimilation was employed to reduce parameter degeneracy and improve identifiability. Second, posterior distributions and parameter correlations were explicitly analyzed rather than relying on single best-fit values. Third, posterior predictive intervals were used to assess how well the inferred parameters reproduce the observed kinetics.

It is important to emphasize that the proposed Bayesian framework complements rather than replaces classical physically motivated identification approaches. Traditional metallurgical methods can extract kinetic parameters such as activation energy and mobility prefactors from carefully designed experiments under simplifying assumptions. The contribution of the present approach is that it allows simultaneous estimation of several physically meaningful parameters, quantifies uncertainty and parameter correlations, and naturally incorporates sequential updating when new measurements become available. The reference parameter set used in the present synthetic study was selected to be consistent with ranges reported in prior MiReX calibrations and experimental recrystallization studies for steels [13], which supports the physical plausibility of the inferred parameter values and suggests that the proposed Bayesian framework can provide physically meaningful estimates when applied to experimental data.

The main limitation of this study is the use of synthetic data. Real experiments will involve additional effects such as measurement noise, material heterogeneity, and possible differences between the model and the actual material behavior. Nevertheless, testing the method under controlled conditions is an important first step. Future work will focus on applying the framework to experimental recrystallization data and incorporating additional observables, such as texture measurements, to improve parameter identifiability and to assess the physical consistency of the inferred parameters.

**Acknowledgement**

This research was carried out under project number N21022e in the framework of the Partnership Program of the Materials innovation institute M2i (www.m2i.nl) and the Netherlands Organization for Scientific Research (www.nwo.nl).

**References**

[1] Y. Seguchi, M. Okugawa, C. Zhu, A. Yamanaka, and Y. Koziumi. Data assimilation for phase-field simulations of the formation of eutectic alloy microstructures. *Comput. Mater. Sci.*, 237:112910, 2024.

[2] A. Yamanaka, Y. Maeda, and K. Sasaki. Ensemble kalman filter-based data assimilation for three-dimensional multi-phase-field model: Estimation of anisotropic grain boundary properties. *Mater. Des.*, 165:107577, 2019.

[3] E. Miyoshi, M. Ohno, Y. Shibuta, A. Yamanaka, and T. Takaki. Novel estimation method for anisotropic grain boundary properties based on bayesian data assimilation and phase-field simulation. *Mater. Des.*, 210:110089, 2021.

[4] T. Fujiwara, E. Miyoshi, and A. Yamanaka. Evaluating inclination-dependent anisotropic grain boundary energies: Bayesian data assimilation approach using molecular dynamics and phase-field simulations. *Comput. Mater. Sci.*, 248:113605, 2025.

[5] A. Ishii, A. Yamanaka, M. Yoshinaga, S. Sato, M. Ikeuchi, H. Saito, S. Hata, and A. Yamamoto. High-fidelity phase-field simulation of solid-state sintering enabled by bayesian data assimilation using in situ electron tomography data. *Acta Mater.*, 278:120251, 2024.

[6] M. Ohno, Y. Oka, S. Sakane, Y. Shibuta, and T. Takaki. Bayesian inference of solid-liquid interfacial properties out of equilibrium. *Phys. Rev. E*, 101(5):052121, 2020.

[7] P. Honarmandi and R. Arroyave. Using bayesian framework to calibrate a physically based model describing strain-stress behavior of trip steels. *Comput. Mater. Sci.*, 129:66–81, 2017.

[8] P.J. Van Leeuwen. Nonlinear data assimilation in geosciences: an extremely efficient particle filter. *Q. J. R. Meteorol. Soc.*, 136(653):1991–1999, 2010.

[9] P. Fearnhead and H.R. Künsch. Particle filters and data assimilation. *Annu. Rev. Stat. Appl.*, 5(1):421–449, 2018.

[10] C. Grudzien and M. Bocquet. A tutorial on bayesian data assimilation. *arXiv preprint arXiv:2112.07704*, 2021.

[11] A. Murakami, T. Shuku, S. Nishimura, K. Fujisawa, and K. Nakamura. Data assimilation using the particle filter for identifying the elasto-plastic material properties of geomaterials. *Int. J. Numer. Anal. Methods Geomech.*, 37(11):1642–1669, 2013.

[12] S.B. Harris, R. Fajardo, A.A. Puretzky, K. Xiao, F. Bao, and R.K. Vasudevan. Bayesian state estimation unlocks real-time control in thin film synthesis. *arXiv preprint arXiv:2410.23895*, 2024.

[13] A. Mathevon, V. Massardier, D. Fabrègue, P. Rocabois, and M. Perez. A microstructurally based model for recrystallization in dual-phase steels. *Metall. Mater. Trans. A*, 51(8):4228–4241, 2020.